RECONSTRUCTION OF MICROWAVE ABSORPTION PROPERTIES IN HETEROGENEOUS TISSUE FOR MICROWAVE-INDUCED THERMO-ACOUSTIC TOMOGRAPHY

J.-G. Wang[1], Z.-Q. Zhao[1, *], J. Song[1], X.-Z. Zhu[1], Z.-P. Nie[1], and Q.-H. Liu[2]

[1]School of Electronic Engineering, University of Electronic Science and Technology of China, Chengdu, Sichuan 611731, China

[2]Department of Electrical and Computer Engineering, Duke University, Durham, NC 27708, USA

Abstract—Aiming to efficiently overcome the acoustic refraction and accurately reconstruct the microwave absorption properties in heterogeneous tissue, an iterative reconstruction method is proposed for microwave-induced thermo-acoustic tomography (MITAT) system. Most current imaging methods in MITAT assume that the heterogeneous sound velocity (SV) distribution obeys a simple Gaussian distribution. In real problem, the biological tissue may have several different inclusions with different SV distribution. In this case, the acoustic refraction must be taken into account. The proposed iterative method is consisted of an iterative engine with time reversal mirror (TRM), fast marching method (FMM) and simultaneous algebraic reconstruction technique (SART). This method utilizes TRM, FMM and SART to estimate the SV distribution of tissue to solve the phase distortion problem caused by the acoustic refraction effect and needs little prior knowledge of the tissue. The proposed method has great advantages in both spatial resolution and contrast for imaging tumors in acoustically heterogeneous medium. Some numerical simulation results are given to demonstrate the excellent performance of the proposed method.

1. INTRODUCTION

Microwave-induced thermo-acoustic tomography (MITAT) has recently received more and more attentions because of its great potential in biomedical applications [1–4]. The basic idea of the MITAT is that a microwave pulse heats a tissue sample, and then the sample absorbs the microwave energy and simultaneously generates temporal thermo-acoustic waves. An image of the electromagnetic absorption distribution is reconstructed from the received thermo-acoustic signals [5]. This image reveals the physiological and pathological status of the tissue, which can be very useful in many applications. Due to its safety and low cost imaging, MITAT has great potential in early tumor detection [5]. Compared with other acoustic imaging systems and microwave systems, the MITAT system has the advantages of both high spatial resolution and high contrast.

Various reconstruction methods for acoustically heterogeneous medium in MITAT have been reported. Hristova et al. [6–8] applied time reversal mirror (TRM) to reconstruct the image under the assumption that the sound velocity (SV) distribution of heterogeneous media is known. However in engineering the SV distribution of the heterogeneous medium is usually unknown. Hristova et al. also pointed out that the using of an incorrect SV distribution would deteriorate both the amplitudes, as well as the locations of the features of the image [6]. In order to overcome this problem, some improved methods have been approached. [9] and [10] proposed a correction method based on ultrasonic transmission tomography (UTT) to measure the SV distribution in the tissue beforehand. It would be extremely valuable to recover the image of the electromagnetic absorption distribution from the measured data without any additional measurements. Zhang and Anastasio [11] proposed a method for reconstructing both the acoustic speed and electromagnetic absorption distribution of the tissue. But this method assumes that the interface geometry of the SV distribution of the tissue is known and also needs some prior knowledge about the SV distribution of the tissue. Xie et al. [12] presented an adaptive and robust method of reconstruction for thermo-acoustic tomography, which suits for weakly heterogeneous tissue. The SV distribution of the heterogeneous tissue in their model is assumed to be a Gaussian distribution. As summarized in their paper [12], this method does not consider the acoustic refraction effect resulted from the heterogeneous SV distribution. Cox and Treeby [13] utilized TRM to reconstruct the weakly heterogeneous tissue and demonstrate the robustness of TRM. They also assume that the heterogeneous tissue obeys a Gaussian distribution and ignores the acoustic refraction.

Actually, the SV distribution of the biological tissue does not obey a simple Gaussian distribution. In this realistic situation, the acoustic refraction must be taken into account. A numerical study showed that the effects of the acoustic refraction can be reduced by using SV distribution [9, 10, 14]. Hence, it is very important to extract the information of the SV distribution of the heterogeneous biological tissue from the measured data. An energetic algorithm for solving the SV distribution is the fast marching method (FMM) based on simultaneous algebraic reconstruction technique (SART) [15, 16]. (For convenience, we note the FMM based on SART as FMM-SART algorithm). FMM-SART algorithm has been applied in ultrasound computed tomography (UCT) [17–20] and has excellent performance in solving the SV distribution.

In this paper, we propose a new iterative method based on the TRM technique and FMM-SART algorithm to accurately reconstruct the microwave absorption properties for MITAT when the acoustic refraction is taken into account. The proposed iterative reconstruction method firstly sets an initial homogeneous SV distribution to approximate the real SV distribution of the tissue. Then it makes use of the TRM and FMM-SART algorithm to iteratively correct the SV distribution. Finally the microwave absorption distribution image is reconstructed by using TRM technique based on the latest updated SV distribution. This method corrects the acoustic refraction effects in heterogeneous tissue by estimating the SV distribution. It greatly enhances the spatial resolution and image contrast. Furthermore, the proposed method only uses the measured data and needs little prior information of the tissue.

The remainder of the paper is organized as follows. Section 2 describes the proposed iterative reconstruction method. Some simulation results and discussions are given in Section 3. Excellent performance of the iterative reconstruction method is demonstrated. Conclusions are drawn in the final section.

2. ITERATIVE RECONSTRUCTION METHOD

2.1. Problem Formulation

In MITAT system, the thermo-acoustic forward problem can be written as follows [6–10, 13]:

$$
\begin{cases}
\left[\frac{\partial^2}{\partial t^2} - v(m)^2 \rho(m) \nabla \cdot \left(\frac{1}{\rho(m)} \nabla \right) \right] p(m, t) = 0, \\
p(m, t) \mid_{t=0} = P_0(m), \quad \frac{\partial p(m,t)}{\partial t} \mid_{t=0} = 0,
\end{cases}
\tag{1}
$$

where $p(m, t)$ is the acoustic pressure at time t and location $m \in \Omega$ inside the 2-D imaging region Ω, $\rho(m)$ the density, and $v(m)$ the SV distribution of the tissue. Both $\rho(m)$ and $v(m)$ may vary with position m. $P_0(m)$ is the original pressure distribution and roughly proportional to the microwave energy absorption distribution.

The thermo-acoustic image reconstruction problem is to estimate $P_0(m)$ from the given measured data $p(m_s, t)$ on an arbitrary measurement surface S, where $m_s \in S$. However, most current imaging methods in MITAT assume that the heterogeneous SV distribution obeys a Gaussian distribution. But in practice, there may have several other different tissues embedded in the biological tissue, which have different SV distributions. The current methods will not work well. For this situation, the acoustic refraction must be considered. The goal of the proposed method is to solve the phase distortion problem caused by acoustic refraction and accurately reconstruct the microwave absorption properties.

In the following, first some brief introductions on both TRM and FMM-SART algorithm will be given, and then an iterative reconstruction method for MITAT will be described in detail.

2.2. TRM Technique in MITAT

The application of TRM to tomography was initially suggested by Xu and Wang [21]. A great deal of work has been done to demonstrate that TRM technique could be used as an imaging algorithm for MITAT [22–25].

The main idea of the TRM is that according to the measured data on measurement surface S, reverse the time and solve the following equations:

$$\begin{cases} \left[\frac{\partial^2}{\partial \tilde{t}^2} - \tilde{v}^2(m)\tilde{\rho}(m)\nabla \cdot \left(\frac{1}{\tilde{\rho}(m)}\nabla \right) \right] \tilde{p}\left(m, \tilde{t}\right) = 0, \\ \tilde{p}\left(m, \tilde{t}\right)|_{\tilde{t}=0} = 0, \ \frac{\partial \tilde{p}(m,\tilde{t})}{\partial \tilde{t}}|_{\tilde{t}=0} = 0, \\ \tilde{p}\left(m_s, \tilde{t}\right) = p\left(m_s, T - \tilde{t}\right), \end{cases} \quad (2)$$

where the reverse-time variable $\tilde{t}$ runs from 0 to T, and the symbol m_s represents the sensor positions on an arbitrary measurement surface. At time $\tilde{t} = T$, the solution of (2) equals to the original pressure $P_0(m)$. (A detailed mathematical derivation process of TRM can be referred in [6, 7, 21, 22].)

From (2), we can see that the solution to (2) will not be equal to $P_0(m)$ if $\tilde{v}(m)$ and $\tilde{\rho}(m)$ in (2) is not equal to $v(m)$ and $\rho(m)$ in (1). Actually, $\tilde{v}(m)$ and $\tilde{\rho}(m)$ are usually selected as a spatially-averaged value of $v(m)$ and $\rho(m)$ [12, 13]. So the pressure reconstructed by TRM

is just an approximate solution of $P_0(m)$. Cox and Treeby [13] have demonstrated that TRM still works well for this situation that the SV distribution of the tissue obeys Gaussian distribution. However, it will not be robust when the acoustic refraction is taken into consideration. One must obtain some information of the real SV distribution to overcome the acoustic refraction effect.

2.3. FMM-SART Algorithm

FMM-SART algorithm refers to a standard ultrasound problem, with well identified sources and receivers. It combines FMM with SART to estimate the real SV distribution of the biological tissue. FMM-SART algorithm has been done on experimental demonstrations and simulations in UCT [18]. This approach can be described in brief as follows.

A key mathematical equation in ray theory is the Eikonal equation which is reformulated in 2-D as:

$$\left[(\partial U/\partial x)^2 + (\partial U/\partial y)^2\right] = 1/v^2(x, y), \tag{3}$$

where $v(x, y)$ is the SV value at pixel (x, y), and $U(x, y)$ is the time-of-flight (TOF) from the source to the pixel (x, y).

For given SV distribution, FMM can efficiently solve (3) and calculate the TOF at each pixel (x, y). Then FMM calculates the fastest propagation path from the receiver back to the source according to the gradients of the calculated TOFs. Therefore, the TOFs calculated by using FMM at receivers will be equal to the TOFs evaluated from the measured data if the assumed SV distribution is equal to the real SV distribution.

However, the real SV distribution is actually unknown and the SV distribution initialized can not be equal to the real SV distribution. For this reason, some differences must exist between the TOFs calculated from the measured data and the TOFs simulated by FMM. SART algorithm is therefore applied. SART is an algebraic reconstruction approach, which attempts to update the initial assumed SV distribution $v(x, y)$ towards to the real SV according to these different TOFs by iteratively solving the following pixel update equation [15, 18]:

$$v^k(x, y) = \frac{d}{\dfrac{d}{v^{k-1}(x, y)} + \sum_{i}^{n} \Delta U_i/n}, \tag{4}$$

where k enumerates the iteration. d is the length of one grid and n the number of rays updating the given pixel (x, y). The expression of ΔU_i

is given as:

$$\Delta U_i = (TOF_{col}(i) - TOF_{sim}(i))/L, \tag{5}$$

where the $TOF_{sim}(i)$ is the TOF calculated by FMM at the position of ith transducer based on the assumed SV. L is the number of the pixels included by the ray path from the given source to the ith transducer. The $TOF_{col}(i)$ is the TOF picked from the received data of ith transducer.

2.4. Iterative Method for MITAT

The problem in MITAT is somewhat different from that in UCT. In UCT, ultrasound signal is emitted from one transducer to biological tissue and other transducers receive the ultrasonic signals. In MITAT, however, ultrasonic signals are generated by thermo expansion in biological tissue. In one word, the acoustic source in UCT is known; nevertheless the acoustic source in MITAT is unknown, which limits the application of FMM-SART algorithm.

A key contribution of this paper is that we combine TRM with FMM-SART to compensate for their defects to solve the inverse problem in MITAT. First TRM technique is used to estimate a preliminary source position based on the initial assumed SV distribution. Second FMM is applied to calculate all the TOF_{sim}s and the propagation paths according to the estimated source position and the initial assumed SV distribution. Third SART is used to iteratively correct the SV distribution. The processes continue until the difference between the TOF_{col}s and the TOF_{sim}s becomes smaller than a threshold. Finally, an image is reconstructed by using TRM based on the latest updated SV distribution.

Updating the SV distribution is also an important process of the proposed method and has some differences to that in UCT [16, 18]. Because SART updates the SV distribution along the fastest propagation path, the estimated SV distribution will be more close to the real SV distribution as the transducer number increases. In UCT, if we assume that there are M transducers, that every transducer emits once, and that the other $(M - 1)$ transducers receive, one complete iteration will update the SV distribution $M \cdot (M - 1)$ times by using SART algorithm. In MITAT, however, it only updates the SV distribution $N \cdot M$ times where N is the number of the acoustic sources (tumors) in the tissue. Usually, N is far less than M, which can lead to lots of pixels apart from the propagation paths not been updated. Therefore, the transducers are needed as many as possible in MITAT to update all the pixels. In order to update all the pixels with

fewer transducers, we update the pixels not only in the propagation paths but also near around the propagation paths.

The proposed iterative method consists of the following steps:

1) Extract the TOF_{col}s from the received acoustic data.

2) Initialize the SV field and suppose the initial SV field is homogeneous.

3) Estimate the source position by TRM technique based on the current SV field.

4) Calculate TOF_{sim}s at all detectors using FMM based on the current SV field and the source position estimated in step 3).

5) Compute the propagation paths from the source position described in step 3) to all detectors and the corresponding L of each path.

6) Calculate all the correction factors according to (5).

7) Judge whether ΔU_i described in step 6) is smaller than a threshold or not. If all ΔU_i are smaller than the threshold, then reconstruct image using TRM based on the current SV field. If not, update the SV field combining SART and repeat step 3) to step 7).

In step 1), in order to facilitate the calculations of TOF, a TOF picker is applied to automatically calculate the TOFs. The TOF picker combines the wavelet transform and Akaike information criteria (AIC), which is called wavelet-AIC TOF picker. It has been applied to in *vivo* ultrasound breast data. (More details can be found in [26, 27]).

The computational complexity of the proposed method is not serious in 2-D breast model. However, this problem gets very bad in 3-D breast model, which needs to adopt Graphic Processing Units (GPU) [28] or other techniques to speed up tomographic processing in 3-D tomography.

Another important issue is the convergence of the proposed iterative method. Because the proposed method utilizes SART to iteratively update the SV distribution, the convergence of the proposed method is determined by that of SART. The convergence of the SART has been demonstrated by Jiang and Wang [29].

3. NUMERICAL SIMULATIONS

In this section, the performance of the proposed method will be demonstrated by using numerical simulated data. In these simulations, we mainly consider the process that the induced thermo-acoustic signals propagate in the tissue and are received by ultrasound transducers.

Table 1. Nominal dielectric properties of breast tissues.

|	Fatty Breast Tissue	Glandular Tissue	Tumor
Permittivity (F/m)	9	11–15	50
Conductivity (S/m)	0.4	0.4–0.5	4
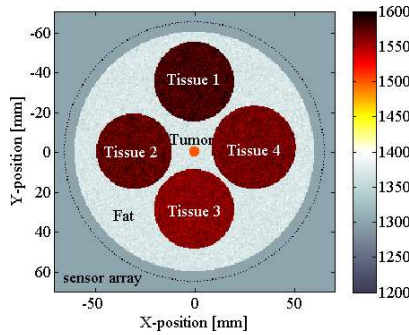
Figure 1. 2-D breast model.

The nominal dielectric properties of breast tissues are listed in Table 1 [12, 30]. The dielectric properties of fatty breast tissue and glandular tissue are very close to each other. So, we assume that the dielectric properties of healthy adipose-dominated tissues are homogeneous approximately but their acoustic parameters are heterogeneous [15, 18]. However, the dielectric properties of tumor are much larger than the fatty breast tissue and glandular tissue. The conductivity between tumor and healthy adipose-dominated tissues in the breast is as large as 10 : 1, which means that the microwave energy absorbed by tumor is 10 times more than that by healthy adipose-dominated tissues. Hence, we assume that tumor is the acoustic source and that the other four tissues do not emit acoustic signals.

A simulation setup about the SV distribution of biological tissue is shown in Fig. 1. A 5-mm-diameter inclusion (located at $X = 0\,\mathrm{mm}$, $Y = 0\,\mathrm{mm}$) is the thermo-acoustic source, which induces acoustic signals. To validate the performance of the proposed method, we set four different sizes of circle areas, which represent the glandular tissues, embedded in the fat. Actually, the SV distribution and density vary spatially in the tissue even in the same tissue. Therefore, the SV values of these five tissues are modeled as 2-D Gaussian distribution with the standard deviation of 10 and the corresponding spatially-

Table 2. Parameters setup.

	Fat	Tissue 1	Tissue 2	Tissue 3	Tissue 4
Velocity (m/s)	1370	1580	1572	1560	1566
Diameter (mm)	120	40	38	40	42
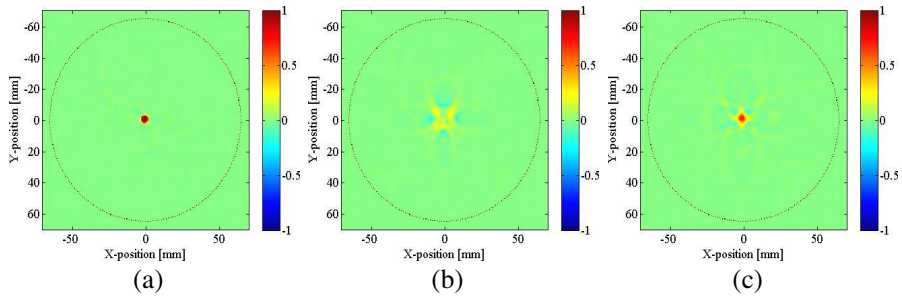
Figure 2. (a) Image reconstructed by TRM with real SV distribution; (b) Image reconstructed by TRM with initial assumed homogeneous SV distribution; (c) Image reconstructed by the proposed method.

averaged SV values and the sizes are given in Table 2. (These SV values are set according to [15] and [18]). The density is selected as $\rho = 0.893 * SV - 349$, which is a relation derived from the measured properties of soft tissue [31]. Moreover, the spatial distribution of inclusions in the tissue is also unknown in practice. So, in all the examples given below, the propagation model based on (1) with varying SV and density is used to simulate the realistic measured data and a similar model based on (2), but with constant homogeneous SV and density is used to reconstruct 256×256 images [32, 33]. 256 ultrasound transducers are put surrounding the biological tissue to receive the ultrasonic signals [15, 18]. The breast model is immersed in a lossless liquid with permittivity similar to that of the fatty tissue [12].

3.1. Without Noise

Though the real SV distribution and density of the tissue are unknown, the spatially-averaged values of SV and density of the tissue are known (as is typically the case in practice) [12, 13]. In this example, the initial assumed SV distribution of biological tissue is homogeneous and the SV value is set to $1370 \, \text{m/s}$. The density is $945.85 \, \text{kg/m}^3$.

The performances of TRM and the proposed method are compared

in Fig. 2. Fig. 2(a) is the image of pressure reconstructed by TRM under the real SV and density distribution. It is used as a reference here. Fig. 2(b) is the image reconstructed by TRM under the assumed constant SV and density distribution. It shows clearly that the acoustic phase is distorted seriously due to the effects of acoustic heterogeneities. Due to the phase distortion, the image is blurred and the image contrast is decreased. Fig. 2(c) is the image reconstructed by the proposed iterative method with one time of iteration. It can be seen that most of the acoustic signals are refocused at the right source position in Fig. 2(c) and can easily detect the tumor embedded in the tissue. Fig. 2(c) is not as good as Fig. 2(a), but much better than Fig. 2(b). In Fig. 2, the three images are normalized by original pressure intensity of the tumor.

From Fig. 2, TRM has excellent performance when the real SV distribution of the tissue is known, which need other additional measurement technique to obtain in prior. And this is always nonrealistic. In practice, the real SV distribution of the tissue is always unknown. Conventional TRM will not be able to solve the phase distortion problem caused by acoustic refraction. Obviously, the proposed method mitigates the phase distortion and greatly enhances the spatial resolution for this situation.

To clearly show the robustness of the proposed method, a profile of the pressure recovered by TRM and the proposed method is given in Fig. 3. The solid line is the original pressure of the acoustic source (tumor) generated by thermal expansion, which is roughly proportional to the absorbed microwave energy. The dashed line and the dash-dot line are the pressures reconstructed by TRM and the proposed method separately. The dashed line corresponds to the pressure in Fig. 2(b) at $Y = 0$ mm and the dash-dot line plots the pressure in Fig. 2(c) at $Y = 0$ mm. From Fig. 3, the pressure reconstructed by traditional TRM is spread around the source position with low amplitude. By using the proposed method, the magnitude of the pressure is nearly 4 times larger than that by TRM, which means that the pressure has gathered much stronger at the source position.

Figure 4 is the comparisons between the TOF_{col}s and the TOF_{sim}s. The solid line represents the TOF_{col}s calculated from the measured data; the dash-dot line and dashed line are the TOF_{sim}s simulated by FMM based on the assumed homogeneous SV distribution ($SV = 1370$ m/s) and the SV distribution updated once respectively. The TOF_{sim}s drawn in dash-dot line is far away from the TOF_{col}s drawn in solid line, which means that the initial assumed homogeneous SV is far too different to the real SV distribution. The proposed method iteratively corrects the initial assumed SV
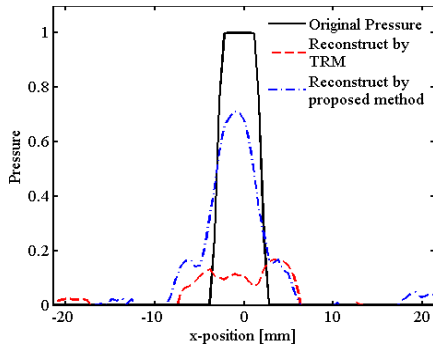
Figure 3. Profiles of the pressure at the source position.
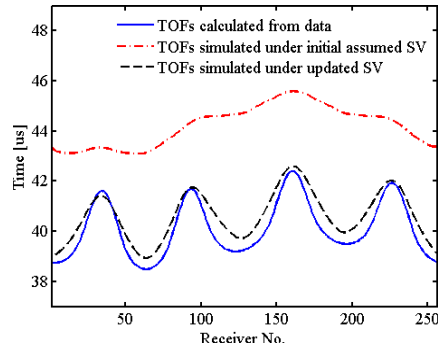
Figure 4. Comparisons between the TOF_{col}s and the TOF_{sim}s.

distribution according to the difference between TOF_{sim}s (the dash-dot line) and TOF_{col}s (the solid line) until the difference between them is less than a threshold. The TOF_{sim}s in dashed line agrees well with the TOF_{col}s in solid line and it means that the updated SV distribution approximates the real SV distribution closely. Therefore, the acoustic signals can be refocused at the source position.

Through this experiment, the advantage of the proposed method has been demonstrated. In the following subsection, its effectiveness will be further tested for the case when the Gaussian noise is introduced.

3.2. With Noise

In order to further demonstrate the robust property of the proposed method, Gaussian noise is added. In [34], 18 dB of signal to noise ratio (SNR) in *vivo* breast data is regarded as low SNR. Here we use 17 dB SNR. The initial assumed SV distribution and density are the same as those in the previous example.

Figures 5(a) and (b) show the images reconstructed by conventional TRM and the proposed method separately, which are also normalized as shown in Fig. 2. Compared with TRM, the proposed method can still recover the original pressure intensity more accurately though the noise is introduced.

Figure 6 gives the profiles of the pressure intensity shown in Fig. 5 at $Y = 0\,\text{mm}$. The solid line is the original pressure intensity, which is generated by thermal expansion and proportional to the absorbed microwave energy. The dashed line and dash-dot line are the pressures recovered at by TRM and the proposed method. Compared with

(a)   (b)
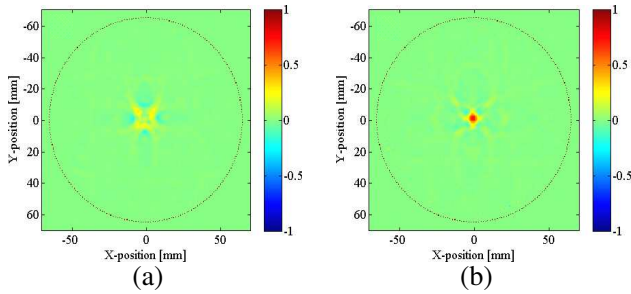
Figure 5. (a) Image reconstructed by TRM; (b) Image reconstructed by the proposed method.
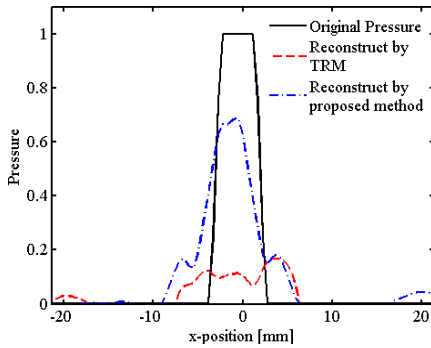
Figure 6. Profiles of the pressure at the source position.
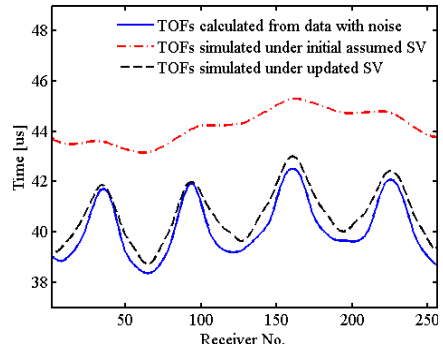
Figure 7. Comparisons between the TOF_{col}s and the TOF_{sim}s.

that in Fig. 3, the pressure reconstructed by the proposed method in Fig. 6 is a little bit worse because of the increasing errors for TOFcols caused by the Gaussian noise. Even though, the proposed method still works better than TRM. It shows that the magnitude of the pressure recovered by the proposed method is more than 3 times larger than that by TRM in this example.

Figure 7 shows the comparisons between the TOF_{col}s and the TOF_{sim}s. The solid line is the TOF_{col}s calculated from the measured data containing random noise. The dash-dot line is the TOF_{sim}s calculated by FMM under the initial assumed homogeneous SV distribution. The dashed line is the TOF_{sim}s calculated by FMM based on the SV distribution updated once. By updating the SV distribution, the TOF_{sim}s drawn in dashed line is closer to the TOF_{col}s. This illustrates that the latest updated SV distribution approximates well to the real SV distribution.

From these examples, it is concluded that the proposed method effectively solves the phase distortion problem induced by acoustic refraction effect via estimating the SV distribution of the tissue. It greatly improves the positioning accuracy and has much higher spatial resolution and contrast of the image than the conventional TRM technique based on the assumption of uniform SV distribution. And due to the TRM engine involved in the proposed method, it also has the advantages of spatial-temporal matched filtering and statistical self-averaging [22–24].

4. CONCLUSIONS

In this paper, a new iterative reconstruction method is proposed for MITAT when the acoustic refraction effect is taken into consideration. The advantages of TRM and FMM-SART algorithms are combined to solve the phase distortion problem in heterogeneous tissue in MITAT. The main idea of the proposed method is that TRM and FMM-SART are iteratively applied to estimate the SV distribution, and the image of microwave absorption is then reconstructed based on the updated SV distribution to overcome the acoustic refraction effect. The effectiveness of the method has been demonstrated by two cases. The results show that the iterative method has better performance than the conventional TRM method in both the spatial resolution and image contrast. The proposed method solves the inverse problem in MITAT using solely measured data with very few acceptable assumptions. Furthermore, this method needs little prior knowledge of the SV distribution of tissue. It might be a promising method in practice.

ACKNOWLEDGMENT

REFERENCES

1. Ku, G., B. D. Fornage, X. Jin, M. Xu, K. K. Hunt, and L. V. Wang, "Thermoacoustic and photoacoustic tomography of thick biological tissues toward breast imaging," *Technol. Cancer Res. Treat.*, Vol. 4, No. 5, 1–7, 2005.
2. Kruger, R. A., P. Liu, Y. R. Fang, and C. R. Appledorn, "Photoacoustic ultrasound (PAUS) — Reconstruction tomography," *Med. Phys.*, Vol. 22, No. 10, 1605–1609, 1995.

3. Ku, G. and L. V. Wang, "Scanning microwave-induced thermoacoustic tomography: Signal, resolution and contrast," *Med. Phys.*, Vol. 28, No. 1, 4–10, 2001.

4. Zeng, X. and G. Wang, "Numerical study of microwave-induced thermo-acoustic effect for early breast cancer detection," *IEEE Antennas and Propagation Society International Symposium*, 839–842, 2005.

5. Xu, M. and L. V. Wang, "Pulsed-microwave-induced thermoacoustic tomography: Filtered backprojection in a circular measurement configuration," *Med. Phys.*, Vol. 29, No. 8, 1661–1669, 2002.

6. Hristova, Y., P. Kuchment, and L. Nguyen, "Reconstruction and time reversal in thermoacoustic tomography in acoustically homogeneous and inhomogeneous media," *Inv. Probl.*, Vol. 24, No. 5, 055006, 2008.

7. Hristova, Y., "Time reversal in thermoacoustic tomography — An error estimate," *Inv. Probl.*, Vol. 25, No. 5, 055008, 2009.

8. Agranovsky, M. and P. Kuchment, "Uniqueness of reconstruction and an inversion procedure for thermoacoustic and photoacoustic tomography," *Inv. Probl.*, Vol. 23, No. 5, 2089, 2007.

9. Jin, X. and L. V. Wang, "Thermoacoustic tomography with correction for acoustic speed variations," *Phys. Med. Biol.*, Vol. 51, 6437–6448, 2006.

10. Jin, X., C. Li, and L. V. Wang, "Effects of acoustic heterogeneities on transcranial brain imaging with microwave-induced thermoacoustic tomography," *Med. Phys.*, Vol. 35, No. 7, 3205–3214, 2008.

11. Zhang, J. and M. A. Anastasio, "Reconstruction of speed-of-sound and electromagnetic absorption distributions in photoacoustic tomography," *Proc. SPIE*, Vol. 6086, 339–345, 2006.

12. Xie, Y., B. Guo, J. Li, G. Ku, and L. V. Wang, "Adaptive and robust methods of reconstruction (ARMOR) for thermoacoustic tomography," *IEEE Trans. Biomed. Eng.*, Vol. 55, No. 12, 2741–2752, 2008.

13. Cox, B. T. and B. E. Treeby, "Artifact trapping during time reversal photoacoustic imaging for acoustically heterogeneous media," *IEEE Trans. Med. Imag.*, Vol. 29, No. 2, 387–396, 2010.

14. Xu, Y. and L. V. Wang, "Effects of acoustic heterogeneity in breast thermoacoustic tomography," *IEEE Trans. Ultrason., Ferroelect. Control.*, Vol. 50, No. 9, 1134–1146, 2003.

15. Li, S., K. Mueller, M. Jackowski, D. Dione, and L. Staib, "Fast

marching method to correct for refraction in ultrasound computed tomography," *IEEE International Symposium in Biomedical Imaging (ISBI)*, 896–899, 2006.

16. Andersen, A. and A. Kak, "Simultaneous algebraic reconstruction technique (SART)," *Ultrason. Imaging*, Vol. 6, 81–94, 1984.

17. Duric, N., P. Littrup, L. Poulo, A. Babkin, R. Pevzner, E. Holsapple, O. Rama, and C. Glide, "Detection of breast cancer with ultrasound tomography: First results with the computed ultrasound risk evaluation (CURE) prototype," *Med. Phys.*, Vol. 34, No. 2, 773–785, 2007.

18. Li, S., M. Jackowski, D. Dione, L. Staib, and K. Mueller, "Refraction corrected transmission ultrasound computed tomography for application in breast imaging," *Med. Phys.*, Vol. 37, No. 5, 2233–2246, 2010.

19. Duric, N., P. Littrup, A. Babkin, D. Chambers, and S. Azevedo, "Development of ultrasound tomography for breast imaging: Technical assessment," *Med. Phys.*, Vol. 32, No. 5, 1375–7386, 2005.

20. Quan., Y. and L. Huang, "Sound-speed tomography using first-arrival transmission ultrasound for a ring array," *Proc. SPIE*, Vol. 6513, 2007.

21. Xu, Y. and L. V. Wang, "Time reversal and its application to tomography with diffracting sources," *Phys. Rev. Lett.*, Vol. 92, No. 3, 1–4, 2004.

22. Fink, M., "Time reversal of ultrasonic fields I. Basic principles," *IEEE Trans. Ferroelectrics, Frequency Control.*, Vol. 39, No. 5, 555–567, 1992.

23. Fink, M. and C. Prada, "Acoustic time reversal mirror," *Inv. Probl.*, Vol. 17, No. 1, 1–38, 2001.

24. Chen, G. P., Z. Q. Zhao, Z. P. Nie, and Q. H. Liu, "A computational study of time reversal mirror technique for microwave-induced thermo-acoustic tomography," *Journal of Electromagnetic Waves and Applications*, Vol. 22, No. 12, 2191–2204, 2008.

25. Chen, G. P., W. B. Yu, Z. Q. Zhao, Z. P. Nie, and Q. H. Liu, "The prototype of microwave-induced thermo-acoustic tomography imaging by time reversal mirror," *Journal of Electromagnetic Waves and Applications*, Vol. 22, No. 11, 1565–1574, 2008.

26. Zhang, H., C. Thurber, and C. Rowe, "Automatic P-wave arrival detection and picking with multiscale wavelet analysis for single-component recordings," *Bull. Seism. Soc. Am.*, Vol. 93, No. 5,

1904–1912, 2003.

27. Ramananantoandro, R. and N. Bernitsas, "A computer algorithm for automatic picking of refraction first-arrival-time," *Geoexploration*, Vol. 24, No. 2, 147–151, 1987.

28. Capozzoli, A., C. Curcio, and A. Liseno, "GPU-based omega-k tomographic processing by 1D non-uniform FFTs," *Progress In Electromagnetics Research M*, Vol. 23, 279–298, 2012.

29. Jiang, M. and G. Wang, "Convergence of the simultaneous algebraic reconstruction technique (SART)," *IEEE Trans. Imag. Proc.*, Vol. 12, No. 8, 2003.

30. Guo, B., Y. Wang, J. Li, P. Stoica, and R. Wu, "Microwave imaging via adaptive beamforming methods for breast cancer detection," *Journal of Electromagnetic Waves and Applications*, Vol. 20, No. 1, 53–63, 2006.

31. Mast, T. D., "Empirical relationships between acoustic parameters in human soft tissue," *Acoust. Res. Lett.*, Vol. 1, No. 2, 37–42, 2000.

32. Cox, B. T., S. Kara, S. R. Arridge, and P. C. Beard, "k-space propagation models for acoustic heterogeneous media: Application to biomedical photoacoustic," *J. Acoust. Soc. Am.*, Vol. 121, No. 6, 3453–3464, 2007.

33. Treeby, B. E. and B. T. Cox, "k-wave: A MATLAB toolbox for the simulation and reconstruction of photoacoustic wave-fields," *J. Biomed. Opt.*, Vol. 15, No. 2, 021314, 2010.

34. Li, C., L. Huang, N. Duric, H. Zhang, and C. Rowe, "An improved automatic time-of-flight picker for medical ultrasound tomography," *Ultrasonic*, Vol. 49, No. 1, 61–72, 2009.